Eur. J. Mineral.
2015, **27**, 521–533
Published online 30 April 2015

Zincian micas from peralkaline phonolites of the Oktyabrsky massif, Azov Sea region, Ukrainian Shield

VICTOR V. SHARYGIN[1,2,*]

[1] V.S.Sobolev Institute of Geology and Mineralogy, Siberian Branch of the RAS, prosp. Akad. Koptyuga 3, Novosibirsk 630090, Russia
[2] Department of Geology and Geophysics, Novosibirsk State University, Pirogova Street 2, Novosibirsk 630090, Russia
*Corresponding author, e-mail: sharygin@igm.nsc.ru

Abstract: Hendricksite, Zn-Mn-bearing fluorophlogopite and phlogopite were observed in the groundmass of two types of peralkaline phonolite from the Oktyabrsky massif, eastern Azov Sea region, Ukraine. These micas are associated with nepheline, potassium feldspar, albite, sodalite, Zn-bearing kupletskite, aegirine, perraultite, fluorite, catapleiite, serandite, *REE*-rich eudyalite, fluorapatite, fluorbritholite-(Ce), a pyrochlore-group mineral, cryolite, thorite, thorianite and a mineral of the cancrinite group. Fine-grained phonolite from the Oktyabrsky massif represents the first known occurrence of hendricksite in peralkaline igneous rocks. This mica is variable in composition (in wt%): SiO_2 (37.7–38.7), TiO_2 (up to 0.3), Al_2O_3 (10.1–10.9), FeO_t (0.3–1.4), ZnO (21.5–25.8), MgO (6.9–9.7), MnO (6.4–7.7), K_2O (8.4–9.1), Rb_2O (0.5–0.8), Li_2O (up to 0.3), F (1.5–2.3) and H_2O (2.1–2.5 wt.%). The simplified average formula of this hendricksite can be expressed as $K(Zn_{1.5}Mg_{0.9}Mn_{0.5}Li_{0.1})(Al_{0.9}Si_{3.1}O_{10})(OH)_{1.5}F_{0.5}$. Zn-Mn-bearing fluorophlogopite and fluorian phlogopite occur in porphyritic phonolite. These micas are richer in SiO_2 (41.5–46.9), MgO (13.2–18.5), Li_2O (0.3–1.3) and F (3.1–5.9), but poorer in Al_2O_3 (7.5–10.0) and ZnO (5.3–15.4 wt%) than hendricksite. Their formulae can be expressed as $K(Mg_2Li_{0.4}Zn_{0.3}Mn_{0.3})(Al_{0.6}Si_{3.4}O_{10})F_{1.3}(OH)_{0.7}$ and $K(Mg_{1.6}Zn_{0.8}Mn_{0.4}Li_{0.2})(Al_{0.8}Si_{3.2}O_{10})(OH)_{1.1}F_{0.9}$, respectively, indicating that these minerals are compositionally intermediate with respect to fluorophlogopite $KMg_3(AlSi_3O_{10})F_2$, phlogopite $KMg_3(AlSi_3O_{10})(OH)_2$, hendricksite $KZn_3(AlSi_3O_{10})(OH,F)_2$ and tainiolite $KLiMg_2(Si_4O_{10})F_2$. The appearance of $^{[6]}$Zn-containing minerals (kupletskite, Zn-rich micas, perraultite) in the Oktyabrsky phonolites indicates low fS_2, high fO_2, high alkalinity and high volatiles content of their parental magma. These rocks represent the latest derivatives of magma evolution for the Oktyabrsky massif. They lack sulphide mineralization and contain abundant H_2O- or F-bearing minerals; their Fe content is mainly concentrated as Fe^{3+} in aegirine.

Key-words: hendricksite; fluorophlogopite; phlogopite; tainiolite; peralkaline phonolite; zinc; mica; Oktyabrsky massif; Ukrainian shield.

1. Introduction

Hendricksite, ideally $K(Zn,Mg,Mn)_3AlSi_3O_{10}(OH)_2$, a Zn-dominant member of the mica group, was first described by Frondel & Ito (1966) and Evans & Strens (1966) in the skarn zones of the Franklin Furnace Mn-Zn-deposit, New Jersey, USA. Since then, this mineral was also identified in Argentina (mine no. 6, San Miguel Group, Córdoba) and Tasmania (Grieves Siding deposit, Oceana mine area, Zeehan). A Zn-rich mica from the latter occurrence was identified by X-ray diffraction (XRD) and has not been verified by chemical data (personal communication from R. Bottrill, Mineral Resources Tasmania). Thus, Zn-dominant trioctahedral micas occur very rarely in nature. However, zincian phlogopite and annite (up to 12.5 wt% ZnO) are common in Mn-Zn skarns and ores of both Franklin Furnace and nearby Sterling Hill (Frondel & Ito, 1966; Frondel & Einaudi, 1968; Craig *et al.*, 1985; Tracy, 1991). A moderate Zn-enrichment (0.2–1.5 wt% ZnO) is also observed in annite, protolithionite and zinnwaldite from some A-type granites and alkaline pegmatites (Stone *et al.*, 1988; Sobachenko *et al.*, 1989; Abdalla *et al.*, 1994; du Bray, 1994; Lowell & Ahl, 2000; Tischendorf *et al.*, 2001, 2007; Brigatti & Guggenheim, 2002; Pekov *et al.*, 2003).

Hendricksite was found in peralkaline fine-grained phonolite from the Oktyabrsky massif, Ukraine (Sharygin *et al.*, 2009). This is the first known occurrence of this mineral in alkaline igneous rocks. Subsequently, Zn-Mn-fluorophlogopite and Zn-Mn-phlogopite were identified by the author in porphyritic phonolite in the same massif. Later, additional analytical data were obtained for the above-mentioned Zn-rich micas; in particular they were analyzed for trace and minor elements and H_2O. The aim of the present study is to discuss the relationships and chemical composition for Zn-rich micas from the Oktyabrsky peralkaline phonolites

0935-1221/15/0027-2460 $ 5.85
DOI: 10.1127/ejm/2015/0027-2460

and general the behaviour of Zn in igneous alkaline environments.

2. Geological background for the Oktyabrsky massif

The Oktyabrsky (formerly, Mariupol) massif is one of the oldest (1.8 Ga) and largest (≈40 km^2) alkaline complexes in the Azov Sea region, Ukrainian shield. The complex is mainly composed of alkaline syenites and foyaites. Nepheline-albite syenites (mariupolites) and their associated pegmatites are minor (Krivdik & Tkachuk, 1988, 1990, 1998). Subalkaline gabbros and their derivates (peridotites, pyroxenites and olivinites) occur in the central part of the massif. Dyke rocks (aegirine microfoyaites, phonolites and nepheline syenite porphyries) are not abundant and predominantly localized outside of the massif in Proterozoic granitoids. The dykes are the latest differentiated products in the Oktyabrsky complex (Krivdik & Tkachuk, 1988, 1998). The majority of alkaline syenites and foyaites within the massif show miaskitic features, (Na + K)/Al = 0.80−0.96 (Dubyna *et al.*, 2014). Nepheline–albite syenites (mariupolites) are miaskitic to agpaitic, and contain accessory minerals (zircon, pyrochlore, fluorbritholite) common in miaskitic nepheline syenites (Krivdik & Tkachuk, 1990; Dumańska-Słowik *et al.*, 2011, 2012, 2015). Only melanocratic nepheline–albite syenites (mariupolites) indicate a peralkaline character, with (Na + K)/Al up to 1.5 due to the abundance of aegirine and Na-feldspathoids. The dyke rocks (aegirine microfoyaites and phonolites) are agpaitic with (Na + K)/Al > 1.1, and occasionally contain eudialyte, catapleiite and astrophyllite-group minerals (Krivdik & Tkachuk, 1988, 1998; Dubina *et al.*, 2008; Sharygin, 2009; Sharygin *et al.*, 2009; Dubyna *et al.*, 2014; Kryvdik *et al.*, 2014).

3. Analytical methods

Double-polished rock sections (~50–100 μm in thickness) were used for optical examination of phonolite samples in transmitted and reflected light. Zn-rich micas strongly resemble Zn-rich kupletskite in their optical and morphological properties, so their preliminary identification was based on energy-dispersive spectra (EDS), back-scattered electron (BSE) images and elemental mapping (EDS system), using JEOL 6380LA, Leo 1430VP and TESCAN MIRA 3MLU scanning electron microscopes at the V.S. Sobolev Institute of Geology and Mineralogy (IGM), Novosibirsk, Russia. The instruments were operated at an accelerating voltage of 20 kV and a probe current of 1 nA in low-vacuum (40–60 Pa) or high-vacuum modes.

Electron microprobe analyses (EMPA), in wavelength-dispersive (WDS) mode, of Zn-micas were obtained at IGM, using a CAMEBAX-micro and a JEOL JXA-8100 electron microprobe. The operating conditions were as follows: beam diameter of 1–2 μm, accelerating voltage of 20 kV, beam current of 15–25 nA, counting time of 10 s (for all elements). A total of 12 elements were measured using the following standards: synthetic fluorophogopite (K, Al, Mg, Si, F), diopside (Ca), rhodonite (Mn), synthetic $ZnFe_2O_4$ (Zn), pyrope (Fe), synthetic $RbNd(WO_4)_2$ (Rb), albite (Na), ilmenite (Ti). Precision for the major elements was better than 2 % relative. Data reduction was performed using a PAP routine (Pouchou & Pichoir, 1985). Overlap corrections were done for the following elements: Si$K\alpha$ – Sr$L\alpha$, Si$K\alpha$ – Rb$L\alpha$, Mn$K\beta$ – Fe$K\alpha$, Mn$L\alpha$ – F$K\alpha$, Fe$L\alpha$ – F$K\alpha$ and Zn$L\alpha$ – Na$K\alpha$. Microprobe analyses were performed on the grains larger than 5 μm. The total Fe content in Zn-mica from the Oktyabrsky phonolite is given as FeO. However, the presence of minor Fe_2O_3 in this mineral cannot be excluded, because the dominant rock-forming pyroxene is aegirine ($NaFe^{3+}Si_2O_6$). All Mn is assumed to be divalent, because associated Mn-rich minerals (kupletskite, serandite, perraultite) contain only MnO.

The contents of some trace elements (Be, Li, B, Rb, Ba, Sr and Cs) and H_2O in micas were analysed by secondary-ion mass spectrometry (SIMS) on a Cameca IMS-4f ion probe at Analytical Centre of the Yaroslavl Branch of the Institute of Physics and Technology, Yaroslavl, Russia. For the analysis, mica blades larger than 20 μm and previously analysed by EMPA were selected. Analysis of trace elements was carried out by the energy-filter method; operating conditions were as follows: primary O^{2-} beam – 20 μm, I = 2–4 nA, energy offset – 100 eV, and energy slit – 50 eV. Concentrations of elements were determined from the ratios of their isotopes to ^{30}Si, using calibration curves for standard samples (Jochum *et al.*, 2000). The hydrogen content was determined from the ^{1}H mass together with trace elements. Low background content of H_2O (0.03 wt%) in the mass spectrometer was achieved by storing the samples for 24 h in a high vacuum. The NIST610 glass was used as external standard.

4. Petrography of peralkaline phonolites

The studied peralkaline phonolites occur 4 km to the north of the Oktyabrsky massif (Kamennaya Gully in upper reaches of the Kalka River). Morozewicz (1930) described them as dyke mariupolitic phonolites. Unfortunately, this area was recultivated and relations between the phonolites and country-rock granites are now obscured. The alkaline rocks presumably form a small plug (50 × 20 m) or a series of dikes crosscutting granites.

Two textural varieties of phonolites are oberved at this locality (Fig. 1, Table 1). The most common one is fine-grained phonolite, which is holocrystalline and massive, and has a grey colour. Rare phenocrysts (up to 5 mm across) and microphenocrysts (<0.5 mm) of potassium feldspar, nepheline and zoned Zn-rich kupletskite are set in the fine-grained groundmass composed of leucocratic minerals (nepheline, K-feldspar, albite, sodalite and a mineral of the cancrinite group) and aegirine. Unfortunately, EMPA data with low totals (88–91 wt%) for the cancrinite-group mineral do not allow for identification. This Na-dominant mineral may be

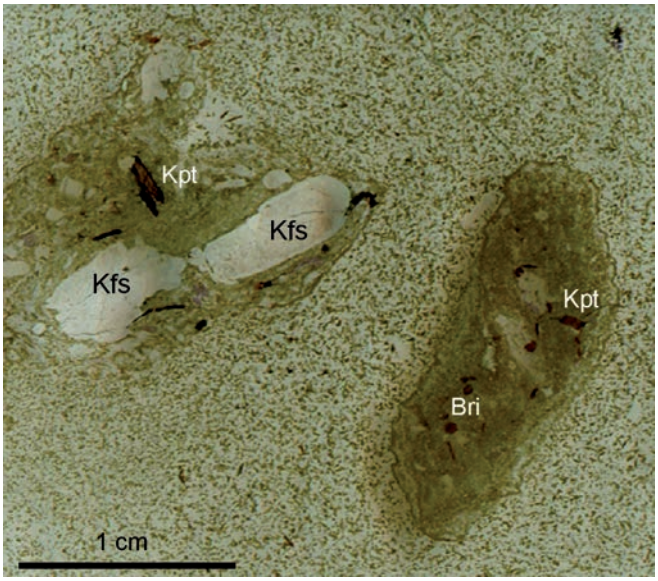

Fig. 1. Porphyritic clasts in fine-grained phonolite, Oktyabrsky massif (microphotograph in transmitted light). Symbols: Kpt – Zn-rich kupletskite; Kfs – potassium feldspar; Bri – fluorbritholite-(Ce). (online version in colour)

intermediate between cancrinite, cancrisilite and hydroxycancrinite (Pekov *et al.*, 2011) or carbobystrite (Khomyakov *et al.*, 2010). The associated minor and accessory phases in the groundmass are Zn-rich kupletskite, fluorite, catapleiite, serandite, a *REE*-Zr-Mn-rich mineral of the eudialyte group, hendricksite, cryolite, fluorbritholite-(Ce), fluorapatite with a Na-*REE*-rich rim, thorianite, thorite, U-*REE*-rich pyrochlore (Sharygin *et al.*, 2009) and perraultite (Kryvdik *et al.*, 2014).

The second rock type is porphyritic and occasionally occurs as small clasts (up to 2–3 cm) randomly distributed in the fine-grained phonolite. In some cases, the clasts are oriented parallel to implicit (hidden) banding in the host rock. The rock is variable with respect to content, size and suite of phenocrysts (up to 50 vol%, size – 2–7 mm, K-feldspar, nepheline, kupletskite, fluorbritholite), which occur in a more melanocratic groundmass than that in the host phonolite (Fig. 1). Some clasts may contain rounded segregations (up 2–3 mm) consisting of mainly aegirine and fluorite. Besides these textural signatures, the porphyritic phonolite differs from the fine-grained type in a greater proportion of F-bearing minerals. The porphyritic variety contains abundant F-bearing phenocrysts and microphenocrysts, including fluorbritholite-(Ce), Zn-rich kupletskite, fluorite and rarely fluorapatite, and groundmass phosphates (fluorapatite with Na-*REE*-rich rim, monazite) and *REE*-fluorocarbonates. In addition, native Cu (mainly as rounded inclusions in fluorapatite), Zn-Mn-F-rich magnesian micas, and Y-*REE*-rich götzenite have been found as accessory phases in the groundmass of this

Table 1. Primary minerals found in fine-grained (1) and porphyritic (2) phonolites.

Mineral	Formula	1	2
Aegirine	$NaFe^{3+}Si_2O_6$	+	+
Nepheline	$Na_3K(AlSiO_4)_4$	+	+
Potassium feldspar	$KAlSi_3O_8$	+	+
Albite	$NaAlSi_3O_8$	+	+
Sodalite	$Na_8Al_6Si_6O_{24}Cl_2$	+	+
''Cancrinite''	$Na_7Al_5Si_7O_{24}(CO_3)\cdot 3H_2O$	+	+
Fluorite	CaF_2	+	+
Cryolite	Na_3AlF_6	+	+
Zn-rich kupletskite	$K_2Na(Mn,Zn,Fe^{2+})_7(Ti,Nb,Zr)_2Si_8O_{26}(OH)_4F$	+	+
Niobokupletskite	$K_2Na(Mn,Zn,Fe^{2+})_7(Nb,Zr,Ti)_2Si_8O_{26}(OH)_4(O,F)$	+	+
Zircophyllite	$K_2(Na,Ca)(Mn,Fe^{2+})_7(Zr,Nb)_2Si_8O_{26}(OH)_4F$	+	+
Perraultite	$(Na,Ca)(Ba,K)(Mn,Zn,Fe)_4(Ti,Nb,Zr)_2(Si_2O_7)_2O_2(F,OH,O)_3$	+	+
Serandite	$Na(Mn,Ca)_2Si_3O_8(OH)$	+	+
Zn-Mn-rich fluorophlogopite	$K(Mg,Zn,Mn)_3(AlSi_3O_{10})(F,OH)_2$		+
Zn-Mn-rich phlogopite	$K(Mg,Zn,Mn)_3(AlSi_3O_{10})(OH,F)_2$		+
Hendricksite	$K(Zn,Mn,Mg,Fe^{2+})_3(AlSi_3O_{10})(OH,F)_2$	+	
''REE-rich eudialyte''	$Na_4(Ca,REE)_2(Mn,Fe^{2+},Y)(Zr,Nb)Si_8O_{22}(OH,Cl)_2$	+	+
Catapleiite	$Na_2ZrSi_3O_9\cdot 2H_2O$	+	
''Y-REE-rich götzenite''	$(Na,Ca,Y,REE)_{3.5}(Ti,Nb)_{0.5}(Si_2O_7)(F,O)_2$		+
U-rich thorianite	$(Th,U)O_2$	+	+
Thorite	$ThSiO_4$	+	
U-*REE*-rich pyrochlore	$(Na,Ca,U,REE)_2(Nb,Ti)_2O_6(OH,F)$	+	+
Fluorapatite	$(Ca,Na,REE)_5(PO_4)_3F$	+	+
Monazite-(Ce)	$(Ce,La,Nd,Th,Ca)(PO_4)$		+
Fluorbritholite-(Ce)	$(Ca,Ce,La,Nd,Na)_5(SiO_4,PO_4)_3(F,OH)$	+	+
Bastnäsite-(Ce)	$(Ce,La,Nd)(CO_3)F$	+	+
Parisite-(Ce)	$Ca(Ce,La,Nd)_2(CO_3)_3F_2$		+
Copper	Cu		+

This Table is based on author's own microprobe and EDS data, and on literature data (Krivdik & Tkachuk, 1988, 1998; Sharygin, 2009; Sharygin *et al.*, 2009; Kryvdik *et al.,* 2014). Mineral names given in *italics* are phases that require further characterization.

phonolite (Table 1). Evidence of secondary alteration in both phonolite types is not very abundant and mainly expressed by the appearance of Zn-rich hydrokupletskite and Mn-hydroxides around Zn-rich kupletskite grains.

The fine-grained phonolites show the following variations in chemical composition (in wt%): SiO_2 54.8–55.3; TiO_2 0.03–0.8; Al_2O_3 18.8–20.2; Fe_2O_3 5.9–6.0; FeO 0.1–1.2; MnO 0.5–0.6; MgO 0.3–0.7; CaO 0.9–1.7; Na_2O 10.8–11.3; K_2O 4.2–4.5; P_2O_5 up to 0.1, F up to 0.4, peralkaline index 1.12–1.25 (Morozewicz, 1930; Krivdik & Tkachuk, 1988). The average contents of selected trace elements are (in ppm): Li – 13; Rb – 405; Sr – 35; Ba – 50; Zr – 3050; Nb – 532; Y – 243; La – 240; Ce – 390; Nd – 235 (Krivdik & Tkachuk, 1998). New determinations (Dubyna *et al.*, 2014) also show high concentrations of Zn (300–400), Ta (30–35); Th (30–45), U (8–11); Pb (25–30) and Be (15–20 ppm).

The existence of two phonolite varieties strongly suggests a two-stage emplacement or crystal fractionation of an initial phonolite melt in a transient magma chamber prior to the emplacement.

5. Zincian micas in phonolites

Hendricksite was identified in the fine-grained phonolite samples. This Zn-rich mica forms brown grains (20–40 μm in length), which are commonly associated with phenocrysts and microphenocrysts of Zn-rich kupletskite (Figs 2 and 3). Discrete small grains (up to 20 μm) and microphenocrysts (up to 150 × 20 μm) of hendricksite rarely occur in the fine-grained groundmass (Fig. 2). The strong chemical difference between mica and Zn-rich kupletskite is clear from both BSE images and elemental maps (Fig. 3). The textural relationships indicate that Zn-rich kupletskite crystallized earlier than hendricksite.

The Zn-Mn-rich fluorophlogopite and phlogopite are observed in porphyritic phonolite clasts. Fluorophlogopite forms colourless bladed microphenocrysts (20 – 50 × 100 – 200 μm) in the groundmass (Fig. 4), whereas phlogopite occurs in aegirine–fluorite segregations (Fig. 5). The relations among the groundmass minerals show that Zn-Mn-rich fluorophlogopite crystallized after aegirine and prior to, or together with Zn-rich kupletskite.

6. Chemical composition

6.1. Hendricksite

The EMPA data for hendricksite from the fine-grained phonolite show the following compositional variation (in wt%): SiO_2 37.7–38.7; TiO_2 up to 0.3; Al_2O_3 10.1–10.9; FeO_t 0.3–1.4; MgO 6.9–9.7; MnO 6.4–7.7; ZnO 21.5–25.8; F 1.5–2.3. Representative analyses are given in Table 2. The examined hendricksite differs significantly

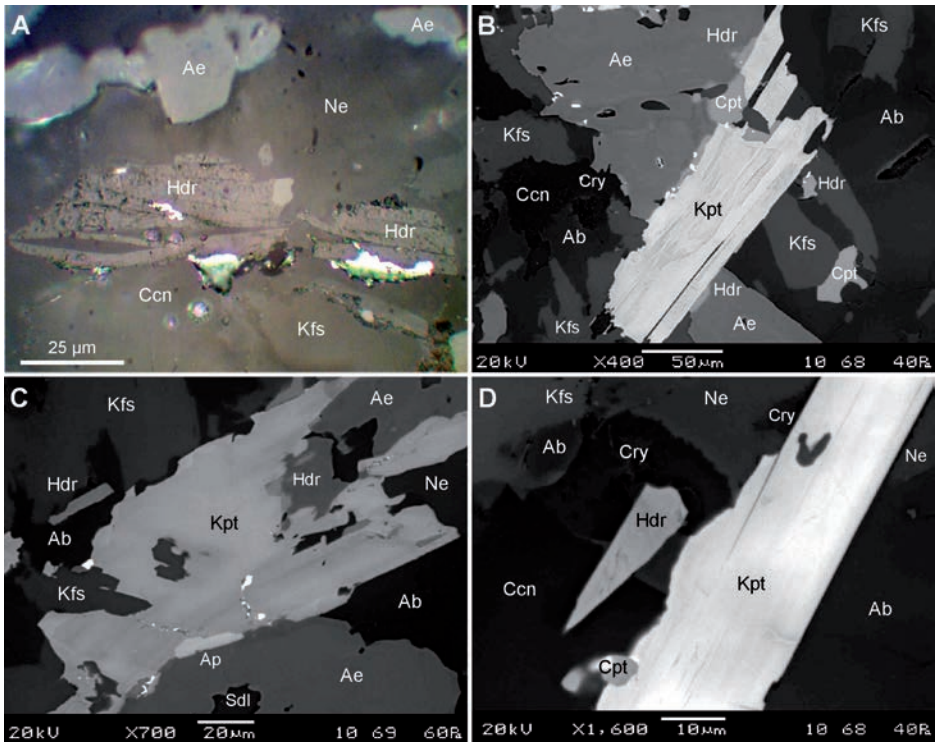

Fig. 2. Hendricksite in fine-grained peralkaline phonolite, Oktyabrsky massif. Symbols: Hdr – hendricksite; Ae – aegirine; Ab – albite; Ne – nepheline; Ccn – a mineral of the cancrinite group; Sdl – sodalite; Cpt – catapleiite; Cry – cryolite; Ap – fluorapatite. For other symbols see Fig. 1. A – microphenocryst (reflected light); B–D – grains near Zn-rich kupletskite microphenocrysts (BSE images). (online version in colour)

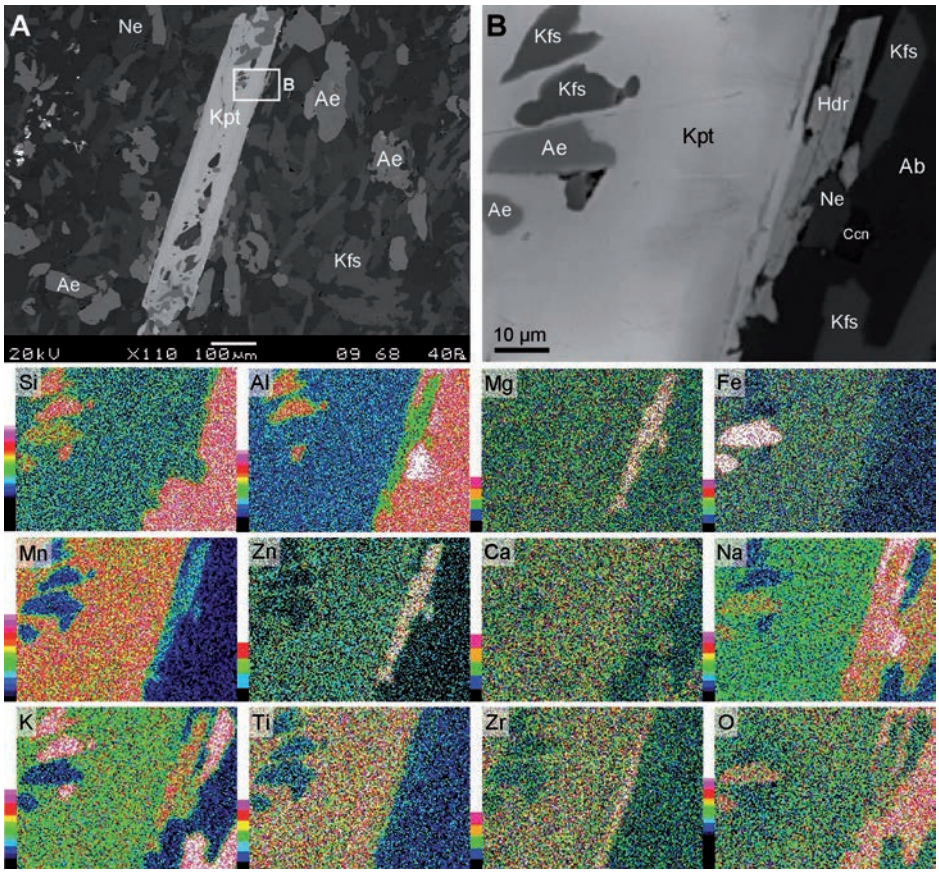

Fig. 3. BSE images and elemental maps for hendricksite overgrown on Zn-rich kupletskite phenocryst in fine-grained phonolite. For symbols see Figs 1 and 2. (online version in colour)

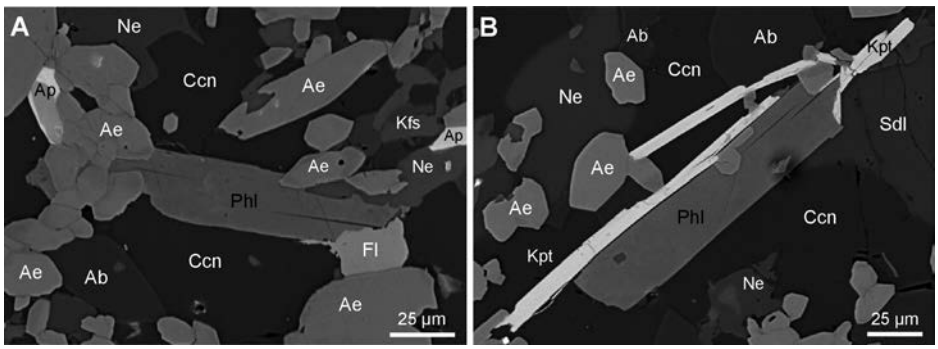

Fig. 4. BSE images of Zn-Mn-bearing fluorophlogopite in the groundmass of a clast of porphyritic phonolite (Okt-2). Phl – Zn-Mn-bearing fluorophlogopite; Fl – fluorite; Ap – fluorapatite with a Na-*REE*-rich rim; for other symbols see Figs 1 and 2.

from the holotype material from Mn-Zn-skarns of Franklin Furnace (Evans & Strens, 1966; Frondel & Ito, 1966; Guggenheim *et al.,* 1983). Most of the Oktyabrsky hendricksite shows relatively little compositional variation. Chemical zoning, observed only in one groundmass microphenocryst, involves a weak increase in Zn and a depletion in Mg, Mn and F from core to rim (Fig. 2A, Table 2, analysis 1). Like Zn-rich kupletskite (Sharygin *et al.*, 2009), the Zn-mica from the fine-grained phonolite contains appreciable amounts of Rb_2O (0.5–0.8 wt%).

The SIMS data confirmed the high concentrations of Rb and F obtained by EMPA (Table 1, analyses 1–2) and showed high levels of H_2O (2.1–2.5 wt%) and Li (1350–1390 ppm), and low levels of other trace elements (in ppm): Ba – 17–33; Cs – 40–66; Sr – 26–66; Be – 14–20; $B < 1$. In comparison, hendricksite from Franklin Furnace shows lower Li_2O (0.04 wt%, Evans & Strens, 1966), but higher BaO contents (0.3–1.3 wt%, Evans & Strens, 1966; Frondel & Ito, 1966; Guggenheim *et al.*, 1983).

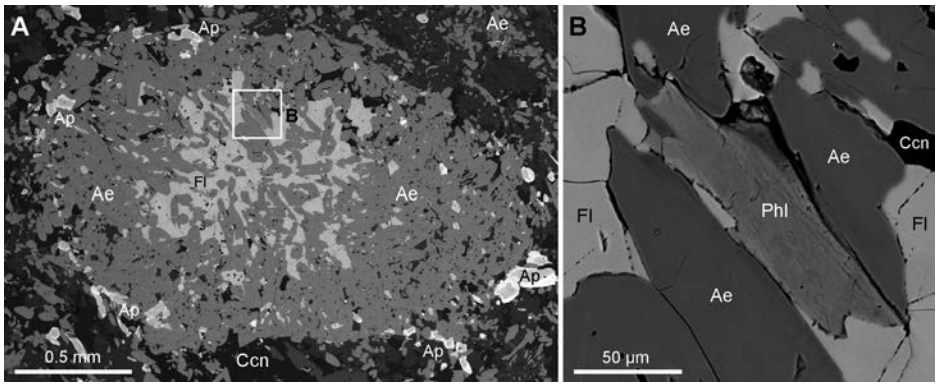

Fig. 5. BSE images of Zn-Mn-bearing phlogopite in an aegirine-fluorite segregation in a clast of porphyritic phonolite (Okt-88). For symbols see Figs1–4.

Among Zn-micas crystal-structure refinement and Raman spectroscopy were provided only for one zincian-manganoan phlogopite (9.38 wt% ZnO, 6.03 wt% MnO) from the Franklin Furnace deposit (Robert & Gaspérin, 1985; Tlili *et al.*, 1989). According to these data, Zn^{2+} occupies exclusively the octahedral sites in the structure, and there is no ordering among six-fold coordinated cations.

Calculations based on 12(O,OH,F) for two complete (EMPA + SIMS) analyses of the Oktyabrsky hendricksite yielded the following formulae:

$$(K_{0.92}Rb_{0.04})(Zn_{1.35}Mg_{1.06}Mn_{0.51}Fe_{0.04}Li_{0.10}Ti_{0.01}Al_{0.07})(Al_{0.91}Si_{3.09}O_{10})(OH_{1.16}F_{0.57}O_{0.27})$$

and

$$(K_{0.92}Rb_{0.04})(Zn_{1.40}Mg_{0.94}Mn_{0.52}Fe_{0.03}Li_{0.10}Ti_{0.02}Al_{0.06})(Al_{0.92}Si_{3.08}O_{10})(OH_{1.38}F_{0.47}O_{0.15}).$$

These calculations indicate some cation deficiency (up to 0.04 apfu) in the interlayer site, minor presence of octahedral Al, and absence of tetrahedral Fe^{3+}. In general, these formulae are consistent with a universal calculation on the basis of 11 oxygens (Table 2), which allowed for estimation of the Li_2O and H_2O contents, where they were not determined analytically.

The simplified average formula of the Oktyabrsky hendricksite may be expressed as $K(Zn_{1.5}Mg_{0.9}Mn_{0.5}Li_{0.1})(Al_{0.9}Si_{3.1}O_{10})(OH)_{1.5}F_{0.5}$, which differs significantly from that of the holotype $K(Zn_{1.5}Mn_{1.0}Mg_{0.5})(AlSi_3O_{10})(OH)_2$ (Evans & Strens, 1966; Frondel & Ito, 1966; Guggenheim *et al.*, 1983). The two hendricksite compositions are probably interrelated via the substitution schemes $Mg^{2+}+F^- \leftrightarrow Mn^{2+}+(OH)^-$ or $Mg^{2+}+Li^+ +Si^{4+}+F^- \leftrightarrow 2Mn^{2+}+Al^{3+}+(OH)^-$. The compositional variations in hendricksite are clearly illustrated in the ternary diagram $(Mg,Fe)^{2+}$–Zn^{2+}–Mn^{2+}, showing the ideal compositions (phlogopite, annite, fluorophlogopite, hendricksite and shirozulite) (Fig. 6), and the plots of Zn *vs.* major elements (Fig. 7). In general, the compositions of hendricksite from both the Oktyabrsky phonolite and the Franklin skarns are far from the ideal $KZn_3(AlSi_3O_{10})(OH,F)_2$, and they cluster near the middle of the hendricksite-phlogopite and hendricksite-shirozulite divides, respectively. This distribution reflects the different substitution schemes operating in the Oktyabrsky hendricksite ($Mg^{2+} \leftrightarrow Zn^{2+}$) and the holotype material [$(Mg,Fe)^{2+} \leftrightarrow (Zn,Mn)^{2+}$] (Figs 6 and 7).

The appreciably high contents of Si in the Oktyabrsky hendricksite can be explained by the following heterovalent substitutions: $^{IV}Al^{3+}+{}^{VI}M^{2+}+2(OH,F)^- \leftrightarrow {}^{IV}Si^{4+}+{}^{VI}Al^{3+}+2O^{2-}$ (Sharygin *et al.*, 2009) or $^{IV}Al^{3+}+{}^{VI}M^{2+} \leftrightarrow {}^{IV}Si^{4+}+{}^{VI}Li^+$, where M^{2+} = Mg, Zn, Mn, Fe.

6.2. Zn-Mn-rich fluorophlogopite and phlogopite

Unlike hendricksite, the Zn-Mn-bearing micas from the porphyritic phonolite clasts are more siliceous and magnesian in composition (in wt%): SiO_2 41.5–46.9; TiO_2 up to 0.3; Al_2O_3 7.5–10.0; FeO_t up to 0.9; MnO 4.0–6.1; ZnO 5.3–15.4; MgO 13.2–18.5; Na_2O up to 0.2; K_2O 9.6–10.5; Rb_2O 0.2–0.6; F 3.1–5.9 (Table 3). In general, these micas can be subdivided in composition into fluorophlogopite (groundmass) and fluorian phlogopite (aegirine–fluorite segregations), which also differ in their Zn content. Compositional zoning is not conspicuous in the BSE images (Figs 4 and 5) due to weak variations in Zn, Mg and Al. The core-to-rim compositions for some discrete grains are given in Table 3.

As in the case of hendricksite, SIMS data were obtained for one grain of fluorophlogopite to confirm the high concentrations of Rb and F measured by EMPA (Table 3, analysis 1). This analysis showed appreciable contents of H_2O (1.2 wt%) and Li_2O (1.26 wt% or 5856 ppm) at low levels of other trace elements (in ppm): Ba – 67; Cs – 19; Sr – 18; Be – 13; B – <1. A calculation based on of 12(O,OH,F) for this complete (EMPA + SIMS) analysis gave the following formula: $(K_{0.96}Na_{0.01}Rb_{0.01})(Mg_{1.97}Zn_{0.32}Mn_{0.26}Li_{0.37}Fe_{0.01}Ti_{0.01}Al_{0.07})(Al_{0.61}Si_{3.39}O_{10})(F_{1.34}OH_{0.54}O_{0.12})$, which in general is consistent with calculation on the basis of 11 oxygens (Table 3).

The simplified average formula of the Oktyabrsky fluorophlogopite can be expressed as $K(Mg_2Li_{0.4}Zn_{0.3}Mn_{0.3})$

Table 2. Chemical composition of hendricksite from fine-grained peralkaline phonolite.

	1			2		3	4	5	6	7	8
	core		rim								
n	*8*	*sd*	*2*	*6*	*sd*	*1*	*2*	*4*	*2*	*4*	*1*
SiO_2 wt%	37.90	0.15	38.01	37.77	0.01	37.48	37.80	37.83	38.04	37.83	31.58
TiO_2	0.11	0.01	0.07	0.25	0.04	0.10	0.15	0.17	0.10	0.16	0.32
Al_2O_3	10.21	0.12	10.19	10.14	0.11	10.44	10.21	10.12	10.39	10.14	13.72
FeO	0.59	0.09	0.47	0.38	0.02	0.50	1.36	0.38	1.11	0.27	2.36
MnO	7.34	0.18	7.04	7.49	0.19	6.49	7.28	7.05	6.35	7.51	12.28
ZnO	22.40	0.61	24.85	23.20	0.65	25.81	24.46	23.04	24.46	23.19	22.97
MgO	8.76	0.60	6.63	7.68	0.23	7.18	6.65	8.67	6.88	7.69	3.69
CaO	0.02	0.01	0.05	0.05	0.01	0.00	0.05	0.01	0.05	0.01	
Na_2O	0.00	0.00	0.00	0.00	0.00	0.02	0.04	0.01	0.07	0.02	0.24
K_2O	8.89	0.17	8.78	8.81	0.08	8.68	8.72	8.50	8.38	8.75	7.91
Rb_2O	0.67	0.05	0.77	0.74	0.04	0.75	0.70	0.75	0.74	0.66	
Li_2O	0.29		*0.25*	0.30		*0.10*	*0.18*	*0.06*	*0.22*	*0.18*	
H_2O	2.13		*2.71*	2.53		*2.86*	*2.86*	*2.89*	*2.89*	*2.74*	3.65
F	2.20	0.35	1.70	1.81	0.08	1.60	1.50	1.62	1.38	1.74	0.45
Sum	101.51		101.52	101.15		102.02	101.92	101.09	101.06	100.88	99.82
$O = F_2$	0.93		0.72	0.76		0.67	0.63	0.68	0.58	0.73	0.19
Sum	100.58		100.80	100.39		101.35	101.29	100.41	100.48	100.15	99.63
Formulae based on 11 oxygens											
Si	3.047		3.106	3.064		3.053	3.080	3.066	3.101	3.087	2.708
Al^{IV}	0.953		0.894	0.936		0.947	0.920	0.934	0.899	0.913	1.292
Sum T	4.000		4.000	4.000		4.000	4.000	4.000	4.000	4.000	4.000
Al^{VI}	0.014		0.087	0.034		0.055	0.060	0.033	0.100	0.062	0.095
Ti	0.007		0.005	0.015		0.006	0.009	0.011	0.006	0.010	0.021
Fe^{2+}	0.040		0.032	0.026		0.034	0.092	0.026	0.076	0.018	0.169
Mn	0.500		0.487	0.514		0.448	0.502	0.484	0.438	0.519	0.892
Zn	1.330		1.499	1.390		1.552	1.472	1.379	1.472	1.397	1.455
Mg	1.050		0.807	0.928		0.872	0.807	1.047	0.836	0.935	0.472
Li	0.094		*0.083*	0.098		*0.033*	*0.058*	*0.021*	*0.072*	*0.059*	
Sum O	3.035		3.000	3.005		3.000	3.000	3.000	3.000	3.000	3.103
Ca	0.002		0.004	0.004		0.000	0.005	0.000	0.004	0.001	
Na	0.000		0.000	0.000		0.004	0.006	0.002	0.012	0.003	0.040
K	0.912		0.915	0.912		0.902	0.906	0.879	0.872	0.910	0.865
Rb	0.035		0.041	0.039		0.039	0.037	0.039	0.039	0.035	
Sum I	0.948		0.960	0.955		0.945	0.953	0.920	0.926	0.949	0.927
OH	1.142		*1.478*	1.369		*1.555*	*1.556*	*1.565*	*1.572*	*1.493*	2.088
F	0.559		0.439	0.466		0.412	0.387	0.414	0.356	0.448	0.122
O^{2-}	0.299		0.083	0.165		0.033	0.058	0.021	0.072	0.059	
Sum cations	7.982		7.960	7.960		7.945	7.953	7.920	7.926	7.949	8.030
End-members, mole %											
$KZn_3[AlSi_3O_{10}](OH,F)_2$	44.15		51.55	47.01		52.83	50.21	46.65	50.87	47.81	48.69
$KMn_3[AlSi_3O_{10}](OH,F)_2$	16.58		16.74	17.40		15.24	17.14	16.36	15.14	17.72	29.86
$KMg_3[AlSi_3O_{10}](OH,F)_2$	28.61		22.06	24.77		27.44	23.60	34.04	23.92	29.90	15.79
$KFe_3[AlSi_3O_{10}](OH,F)_2$	1.32		1.10	0.88		1.17	3.15	0.87	2.62	0.62	5.67
$KMg_2Li[Si_4O_{10}]F_2$	9.34		8.55	9.93		3.33	5.90	2.08	7.44	6.05	

1 – core and rim of microphenocryst (Fig. 2A); 2–4 – small blades around Zn-rich kupletskite microphenocrysts (Figs 2B–D and 3); 5–7 – discrete small blades in the groundmass; 8 – holotype material from Franklin Furnace (Frondel & Ito, 1966). Total includes 0.65 wt% BaO (0.022 apfu Ba). Initial FeO (0.34 wt%) and Fe_2O_3 (2.25 wt%) are recalculated as FeO.
Ba, Sr, Cr and Cl are below detection limits (<<0.01 wt%). *n* – number of analyses. Li_2O and H_2O were determined by SIMS for analyses 1 (core) and 2, for the other analyses calculated values are given in *italic*. Li_2O was estimated as Li (apfu) = 3–ΣO. H_2O was calculated on the basis of total positive charge assuming (OH + F + O) = 2 apfu. Standard deviations (*sd*) are given only for large grains analyzed by SIMS.

$(Al_{0.6}Si_{3.4}O_{10})F_{1.3}(OH)_{0.7}$ (Table 3). This Zn-Mn-rich mica seems to be an intermediate member between fluorophlogopite, $KMg_3(AlSi_3O_{10})(F,OH)_2$, and tainiolite, $KLiMg_2(Si_4O_{10})F_2$. However, compositions strongly enriched in both Zn and Mn have not been previously reported elsewhere for this series (Pekov *et al.,* 2003 and references therein; Armbruster *et al.*, 2007).

In contrast, fluorian phlogopite from the aegirine–fluorite segregation is more significantly enriched in Zn and Mn than the groundmass fluorophlogopite (Table 3, analyses 7–8,

Table 3. Chemical composition of Zn-Mn-bearing lithian fluorophlogopite and phlogopite in clasts of porphyritic peralkaline phonolite.

	1		2		3	4		5	6	7				8
Clast	Okt-2		Okt-2 core	rim	Okt-2	Okt-2 core	rim	Okt-2 core	Okt-2 core	Okt-88 core		rim		ideal
n	*6*	*sd*	*6*	*5*	*7*	*3*	*1*	*2*	*1*	*6*	*sd*	*5*	*sd*	
SiO_2 wt%	46.59	0.30	46.28	46.21	46.27	46.50	45.36	46.56	46.43	42.07	0.60	40.86	0.59	46.43
TiO_2	0.25	0.04	0.29	0.26	0.22	0.45	0.32	0.37	0.27	0.28	0.02	0.23	0.03	
Al_2O_3	7.85	0.28	7.98	8.09	8.32	7.36	8.25	7.84	7.71	9.49	0.30	10.01	0.14	7.30
FeO	0.18	0.05	0.18	0.10	0.15	0.45	0.28	0.54	0.48	0.70	0.11	0.87	0.16	
MnO	4.22	0.20	4.60	4.45	4.37	4.11	4.76	3.94	3.88	5.69	0.14	6.05	0.13	4.06
ZnO	5.92	0.57	5.70	6.29	6.25	5.97	7.71	6.48	6.63	13.83	0.41	15.38	0.50	6.99
MgO	18.17	0.17	17.85	18.02	18.25	18.30	17.34	17.96	17.60	13.87	0.36	13.15	0.52	18.46
CaO	0.00	0.00	0.00	0.00	0.00	0.03	0.06	0.01	0.03	0.09	0.03	0.11	0.03	
Na_2O	0.04	0.03	0.06	0.02	0.09	0.07	0.13	0.13	0.07	0.15	0.10	0.13	0.08	
K_2O	10.33	0.06	10.36	10.37	10.35	10.48	10.44	10.42	10.49	9.94	0.09	9.61	0.10	10.78
Rb_2O	0.26	0.04	0.44	0.42	0.25	0.38	0.40	0.41	0.43	0.52	0.08	0.41	0.04	
Li_2O	1.26		*0.97*	*0.91*	*0.89*	*0.96*	*0.85*	*0.97*	*0.99*	0.70		0.33		1.28
H_2O	1.12		*0.83*	*0.83*	*0.88*	*0.92*	*1.28*	*0.94*	*0.75*	1.98		2.05		1.55
F	5.82	0.08	5.73	5.67	5.63	5.43	4.77	5.39	5.69	3.55	0.18	3.12	0.11	5.44
Sum	102.02		101.19	101.67	101.93	101.40	102.16	101.95	101.25	102.77		102.13		102.29
$O = F_2$	2.45		2.41	2.39	2.37	2.28	2.01	2.27	2.40	1.49		1.32		2.29
Sum	99.57		98.78	99.28	99.56	99.12	100.15	99.68	98.85	101.28		100.81		100.00
Formulae based on 11 oxygens														
Si	3.375		3.422	3.406	3.393	3.430	3.359	3.419	3.439	3.175		3.129		3.375
Al^{IV}	0.625		0.578	0.594	0.607	0.570	0.641	0.581	0.561	0.825		0.871		0.625
Sum T	4.000		4.000	4.000	4.000	4.000	4.000	4.000	4.000	4.000		4.000		4.000
Al^{VI}	0.045		0.118	0.109	0.113	0.069	0.078	0.098	0.112	0.020		0.033		
Ti	0.014		0.016	0.014	0.012	0.025	0.018	0.020	0.015	0.016		0.013		
Fe^{2+}	0.011		0.011	0.006	0.009	0.028	0.017	0.033	0.030	0.044		0.056		
Mn	0.259		0.288	0.278	0.272	0.257	0.299	0.245	0.243	0.364		0.392		0.250
Zn	0.317		0.311	0.343	0.339	0.325	0.421	0.352	0.363	0.771		0.870		0.375
Mg	1.961		1.967	1.979	1.994	2.012	1.913	1.966	1.943	1.561		1.501		2.000
Li	0.367		*0.289*	*0.271*	*0.262*	*0.284*	*0.253*	*0.287*	*0.294*	0.213		0.102		0.375
Sum O	2.973		3.000	3.000	3.000	3.000	3.000	3.000	3.000	2.988		2.967		3.000
Ca	0.000		0.000	0.000	0.000	0.002	0.005	0.001	0.002	0.007		0.009		
Na	0.006		0.008	0.003	0.012	0.010	0.019	0.019	0.010	0.022		0.019		
K	0.955		0.977	0.975	0.968	0.986	0.986	0.976	0.972	0.948		0.922		1.000
Rb	0.012		0.021	0.020	0.012	0.018	0.019	0.019	0.020	0.025		0.020		
Sum I	0.973		1.006	0.998	0.993	1.017	1.029	1.015	1.005	1.002		0.970		1.000
OH	0.541		*0.371*	*0.407*	*0.432*	*0.450*	*0.630*	*0.461*	*0.373*	0.997		1.047		0.750
F	1.332		1.340	1.322	1.307	1.266	1.117	1.252	1.333	0.847		0.754		1.250
O^{2-}	0.127		0.289	0.271	0.262	0.284	0.253	0.287	0.294	0.156		0.199		
Sum cations	7.946		8.006	7.998	7.993	8.017	8.029	8.015	8.005	7.990		7.937		8.000
End-members, mole %														
$KZn_3[AlSi_3O_{10}](OH,F)_2$	10.86		10.85	11.91	11.78	11.20	14.51	12.20	12.62	26.01		29.46		12.50
$KMn_3[AlSi_3O_{10}](OH,F)_2$	8.88		10.04	9.66	9.44	8.84	10.28	8.44	8.47	12.27		13.29		8.30
$KMg_3[AlSi_3O_{10}](F,OH)_2$	42.09		48.45	49.99	51.16	49.70	48.46	48.32	47.32	37.49		41.65		41.70
$KFe_3[AlSi_3O_{10}](OH,F)_2$	0.38		0.38	0.22	0.31	0.95	0.59	1.15	1.03	1.48		1.89		
$KMg_2Li[Si_4O_{10}]F_2$	38.78		30.28	28.22	27.30	29.31	26.16	29.84	30.72	22.75		13.71		37.50

1–6 – core and rim of discrete grains of fluorophlogopite in the groundmass (clast Okt-2, Fig. 4); 7 – phlogopite in an aegirine–fluorite segregation (clast Okt-88, Fig. 5); 8 – ideal composition $K(Mg_2Zn_{0.375}Mn_{0.25}Li_{0.375})[Al_{0.625}Si_{3.375}O_{10}]F_{1.25}(OH)_{0.75}$.

Ba, Sr, Cr and Cl are below detection limits (<<0.01 wt%). *n* – number of analyses. Li_2O and H_2O were determined by SIMS for analyses 1 and 7, for the other analyses calculated values are given in *italic*. Li_2O was estimated as Li (apfu) = 3–ΣO. H_2O was calculated on the basis of total positive charge assuming (OH + F + O) = 2 apfu. Standard deviations (*sd*) are given only for large grains analysed by SIMS.

Fig. 5). SIMS analyses for the core and rim of this grain showed high contents of H_2O (1.98–2.05 wt%), Rb_2O (4717–3762 ppm) and Li_2O (0.70–0.33 wt% or 3246–1540 ppm) at low levels of other trace elements (in ppm): Ba – 77–84; Cs – 27–20; Sr – 11–21; Be – 2–9; B – <1. A calculation based on 12(O,OH,F) for these complete (EMPA + SIMS) analyses yielded the following average formula: $(K_{0.95}Na_{0.02}Rb_{0.02}Ca_{0.01})(Mg_{1.55}Zn_{0.82}Mn_{0.38}Li_{0.16}Fe_{0.05}Ti_{0.02}Al_{0.06})(Al_{0.82}Si_{3.18}O_{10})(OH_{1.03}F_{0.81}O_{0.16})$. Its simplified average formula can be expressed as $K(Mg_{1.6}Zn_{0.8}$

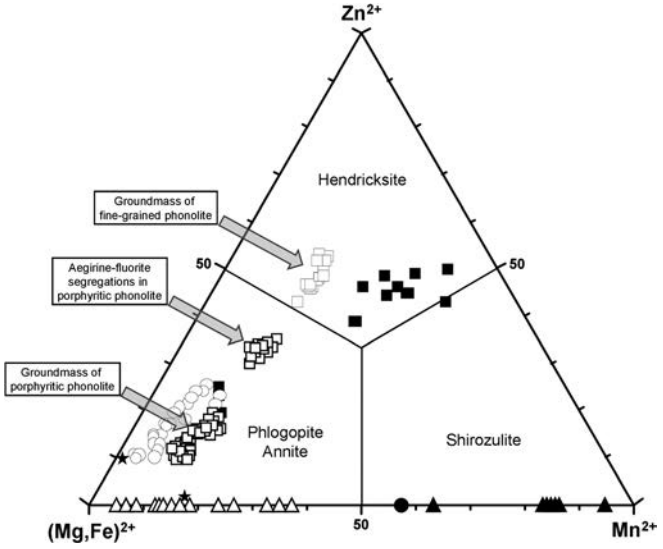

Fig. 6. Compositional variations of Zn-Mn-bearing micas from phonolites of the Oktyabrsky massif in comparison with Zn- and Mn-rich micas from Zn-Mn deposits. Open squares – hendricksite, Zn-bearing fluorophlogopite and phlogopite from phonolites, Oktyabrsky massif, Ukraine (original data); solid squares – hendricksite (holotype) and Zn-bearing phlogopite, Franklin Furnace, NJ, USA (Evans & Strens, 1966; Frondel & Ito, 1966; Guggenheim *et al.*, 1983; Robert & Gaspérin, 1985); open circles – Zn-bearing phlogopite and other Zn-bearing micas, Sterling Hill, NJ, USA (Frondel & Einaudi, 1968; Craig *et al.*, 1985; Tracy, 1991); solid stars – annite (lepidomelane) from nepheline–albite syenites (mariupolites), Oktyabrsky massif (Dumańska-Słowik *et al.*, 2011); solid circle – shirozulite (holotype), Taguchi, Aichi Prefecture, Japan (Ishida *et al.*, 2004); solid triangles – Al-poor ''tetrasilicic'' Mn-mica (shirozulite?), Mn-deposits of South Urals, Russia (Brusnitsyn & Nesterov, 2006); open triangles – manganoan phlogopite (manganophyllite) and annite, Mn-deposits and granites worldwide (Yoshii *et al.*, 1973; Chen & Wu, 1987; Chukhrov, 1992; Tischendorf *et al.*, 2007).

$Mn_{0.4}Li_{0.2})(Al_{0.8}Si_{3.2}O_{10})(OH)_{1.1}F_{0.9}$. The core-to-rim variations (Table 3) show a distinct trend toward hendricksite rather than compositions intermediate between fluorophlogopite and tainiolite.

Thus, the compositional data for Zn-Mn-Mg-bearing micas from the Oktyabrsky phonolites indicate that their enrichment in Si and depletion in Al can be attributed to evolution toward the tainiolite end-member, even for compositions with undetermined Li. Besides hendricksite, shirozulite and tainiolite, both phlogopite and fluorophlogopite are essential components in these micas. The possible compositional relations among the minerals discussed above are shown in Fig. 8.

7. Discussion

7.1. Behaviour of Zn in alkaline magmatic system

The occurrence in alkaline rocks of minerals containing $^{[6]}$Zn in the crystal structure (*e.g.*, kupletskite, hendricksite) indicates low fS_2, high fO_2, high alkalinity (peralkalinity), and high fluid contents in their crystallization environment (Pekov, 2005; Piilonen *et al.*, 2006). Such conditions are most common during the latest crystallization stages in the evolution of large peralkaline magmatic complexes, such as, Khibiny and Lovozero in Russia and Mont Saint-Hilaire in Canada. In this sense, the peralkaline phonolites of the Kamennaya gully are also a remarkable example. These rocks represent the latest magmatic derivatives in the Oktyabrsky massif. They lack sulfide mineralization, and Fe is predominantly accommodated as Fe^{3+} in aegirine. There is a significant modal proportion of silicates containing $^{[6]}$Zn (kupletskite, micas, perraultite), and H_2O- or F-bearing minerals (fluorite, cryolite, fluorbritholite-(Ce), catapleiite, serandite; see Table 1). In the fine-grained phonolite, hendricksite crystallized later than Zn-rich kupletskite, and these minerals recorded a gradual increase in $^{[6]}$Zn and F in the system during crystallization. In the porphyritic phonolite, an increase in F is more drastic, whereas the proportion of $^{[6]}$Zn is similar in both kupletskite and mica. It should be noted that both phonolite types contain abundant fluorite (CaF_2) and cryolite (Na_3AlF_6).

Both kupletskite and mica in the porphyritic phonolite are poorer in ZnO than these minerals in the fine-grained phonolite. Both the phenocryst and groundmass kupletskite in this rock contains 4.4–6.1 wt% ZnO (author's unpublished data), whereas its counterparts from the fine-grained phonolite are richer in ZnO (6.3–7.9 wt%, Sharygin *et al.*, 2009). Hendricksite (with 21.5–25.8 wt% ZnO) is the dominant mica in the fine-grained phonolite, whereas fluorophlogopite and phlogopite from the porphyritic phonolite contain 5.3–15.4 wt% ZnO. Perraultite occurring around kupletskite phenocrysts in the Kamennaya phonolites contains 1.6–2.1 wt% ZnO (Kryvdik *et al.*, 2014). Thus, mica is the preferred phase among all phyllosilicates to concentrate Zn in the Oktyabrsky peralkaline phonolites.

It should be also noted that the high abundance of Na in the parental phonolite melt did not favour accumulation of this element in the micas, as observed in the latest hyperalkaline pegmatites at Khibiny, type locality for shirokshinite $KNaMg_2(Si_4O_{10})F_2$ (Pekov *et al.*, 2003). Sodium-rich tainiolite overgrowing phlogopite was described in marble xenoliths, which were thermally metamorphosed by an alkaline magma at Mont Saint-Hilaire (Armbruster *et al.*, 2007).

Alkali metasomatites at the Dmitrovka open pit and Tunikova gully, which appear to be genetically related to the Oktyabrsky massif, also contain micas and other phyllosilicates. Minerals in the Dmitrovka sulphide-free fenites and albitites are rich in ZnO, but the contents are not significant (in wt%): annite 0.5–2.2; fluorophlogopite 1.6–1.9; tainiolite 0.1–0.3; astrophyllite and ferroan kupletskite 0.6–1.0; kupletskite 1.4–1.6; perraultite 0.8–1.2; jinshajiangite 0.6–0.8; hejtmanite 0.8–0.9; bafertisite 0.5–0.9; arfvedsonite 0.5–1.2. Like in the Kamennaya gully phonolites, the Zn-Mn-F tendency is shown in the Dmitrovka minerals: Mn- and/or F-richer species are more abundant in ZnO (Kryvdik *et al.*, 2010; Sharygin & Kryvdik, 2010, 2014; author's unpublished

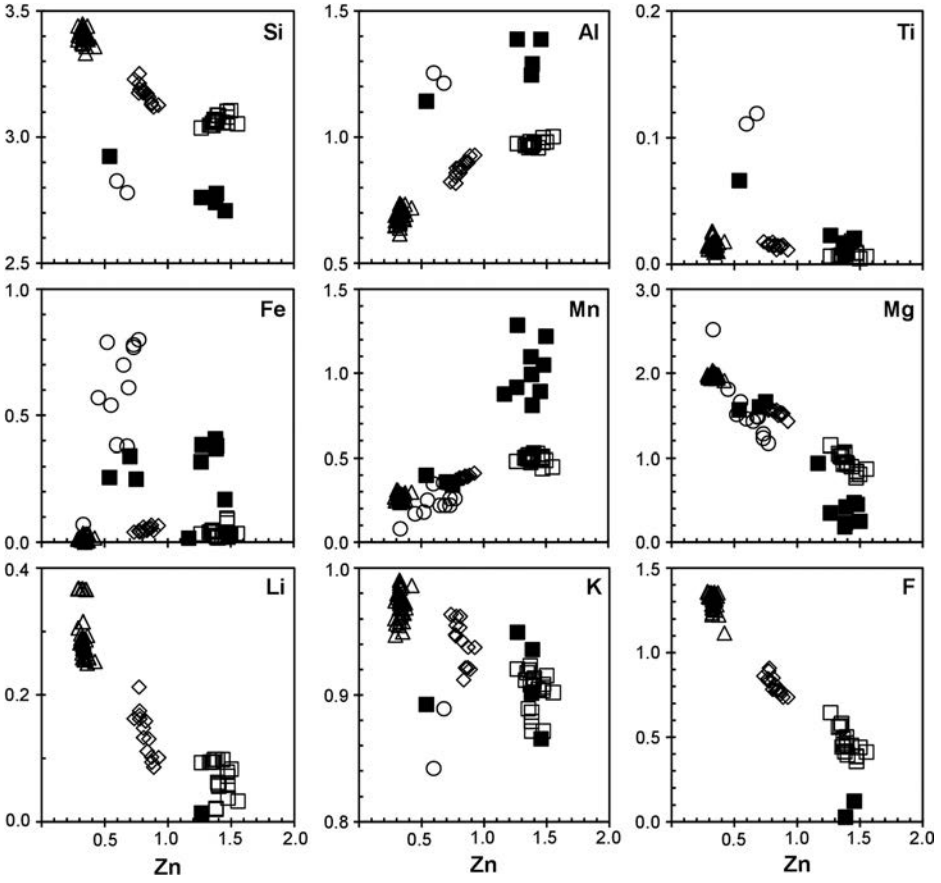

Fig. 7. Variations of Zn vs. major elements (in apfu) for Zn-Mn-bearing micas from phonolites of the Oktyabrsky massif, Ukraine, in comparison with Zn-Mn-rich micas from Franklin Furnace and Sterling Hill, NJ, USA. Open squares – hendricksite from the groundmass of fine-grained phonolite, Oktyabrsky massif; open triangles – Zn-Mn-bearing lithian fluorophlogopite from the groundmass of porphyritic phonolite, Oktyabrsky massif; open rhombuses – Zn-Mn-bearing lithian phlogopite in an aegirine-fluorite segregation of porphyritic phonolite from phonolites, Oktyabrsky massif; solid squares – hendricksite (holotype) and Zn-bearing phlogopite, Franklin Furnace, NJ, USA (Evans & Strens, 1966; Frondel & Ito, 1966; Guggenheim *et al.,* 1983; Robert & Gaspérin, 1985); open circles – Zn-bearing phlogopite, Sterling Hill, NJ, USA (Frondel & Einaudi, 1968; Craig *et al.*, 1985). Calculated and analyzed (SIMS) values of Li in the Oktyabrsky micas are used for the Zn-Li plot.

data). However, in the case of the absence of sulphides, the ilmenite-group minerals are more likely to concentrate Zn in these rocks (up to the appearance of ecandrewsite in the outer part of zoned crystals) (Sharygin & Kryvdik, 2010). In contrast, in fenites at the Tunikova gully, which contain minor sphalerite, the fluorophlogopite and arfvedsonite are virtually free of ZnO (<0.1 wt%). In addition to sphalerite, manganoan ilmenite may accumulate ZnO (5.0–7.5 wt%) in these rocks (Kryvdik *et al.*, 2013). It should be noted that fluorophlogopite from both metasomatic occurrences shows the tendency to evolve toward the tainiolite end-member, but tainiolite as individual mineral appeared only in late associations of the Dmitrovka rocks containing bafertisite- or astrophyllite-group minerals (Sharygin & Kryvdik, 2014).

7.2. Stability of Zn- and Mn-dominant trioctahedral micas

The synthetic end-member compositions $KZn_3(AlSi_3O_{10})(OH)_2$ and $KMn_3(AlSi_3O_{10})(OH)_2$ can be prepared by the hydrothermal techniques from stoichiometric gels and an oxide–$K_2Si_2O_5$ mixture at 1–3 kbar and 250–650°C (Frondel & Ito, 1966; Hazen & Wones, 1972). Perrotta & Garland (1975) synthesized Zn-bearing phlogopite at 55–85°C from gels with a low ZnO concentration. The Mn- and Zn-micas are well crystallized under hydrothermal conditions at 100–200°C (Komarneni & Newalkar, 2003; Choi *et al.*, 2009).

Ishida *et al*. (2004) stated that shirozulite, with the ideal composition $KMn_3(AlSi_3O_{10})(OH)_2$, does not seem to be stable in natural conditions because its octahedral layer is much larger in size than its tetrahedral layer. The Mn^{2+} ion occupying the octahedral sites in this structure has a significantly larger ionic radius (0.83 Å) compared to six-coordinated Mg^{2+} and Fe^{2+} (0.72 and 0.78 Å, respectively, Shannon, 1976). Thus, there are no variants to compensate the difference in the size between the octahedral and tetrahedral layers. Unlike the ideal composition, the holotype shirozulite from Taguchi, Japan (Ishida *et al.*, 2004) is a Mg-rich species with the empirical formula $(K_{0.9}Ba_{0.1})(Mn_{1.5}Mg_{1.0}Fe^{2+}_{0.2}Al_{0.3})(Al_{1.5}Si_{2.5}O_{10})(OH)_2$. The

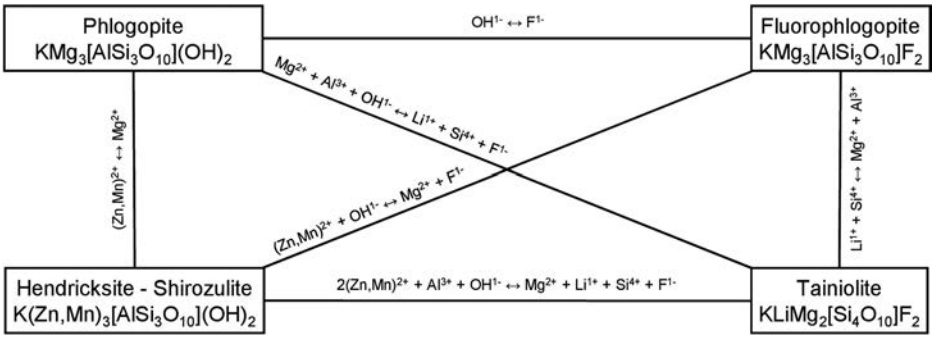

Fig. 8. Isomorphic schemes for Zn-Mn-Mg-Li-containing micas from the Oktyabrsky phonolites within ideal end-members.

additional ^{IV}Al increases the size of the tetrahedral layer, improving linkage between the tetrahedral and octahedral layers. An increasing content of six-coordinated Mg, Fe^{2+}, Al, Li and Fe^{3+} has a similar effect, *i.e.* reducing the dimensions of the octahedral layer. Higher proportions of Mn^{2+} in the octahedral sites (>>50 %) will increase the mismatch between the octahedral and tetrahedral layers. Brusnitsyn & Nesterov (2006) proposed that this mismatch can be compensated via the presence of vacancies in the octahedral layer because of the incomplete occupation according to the isomorphic scheme $^{VI}R^{2+}$ (Mn^{2+}) + $2^{IV}Al^{3+} \leftrightarrow {}^{VI}\square + 2^{IV}Si^{4+}$, which is common in phyllosilicates. This substitution culminates in the ''tetrasilicic'' composition $KMn_{2.5}(Si_4O_{10})(OH)_2$, which is intermediate between the trioctahedral and dioctahedral micas. Brusnitsyn & Nesterov (2006) described Al-undersaturated micas from the Mn deposits of the South Urals (Russia) as shirozulite, but it appears to be a new Mn-member of the mica family and related to montdorite $KFe^{2+}{}_{1.5}Mn^{2+}{}_{0.5}Mg_{0.5}(Si_4O_{10})F_2$ (Robert & Maury, 1979; Melcher, 1995; Rieder *et al.,* 1998).

Thus, the numerous occurrences of manganoan phlogopite (manganophyllite) and annite (Yoshii *et al.*, 1973; Chen & Wu, 1987; Chukhrov, 1992; Tischendorf *et al.*, 2007) and the discovery of magnesian shirozulite (Ishida *et al.*, 2004) strongly suggest the existence of a limited solid solution between phlogopite (annite) and shirozulite, with a miscibility gap close to the composition $KMn_3(AlSi_3O_{10})(OH)_2$.

In the end-member hendricksite, $KZn_3(AlSi_3O_{10})(OH)_2$, the octahedral ionic radius of Zn (0.74 Å) is intermediate between Mg^{2+} and Fe^{2+} (Shannon, 1976). Therefore, the existence of the complete solid solutions between phlogopite (or annite) and hendricksite is very likely. The Zn-bearing micas from the Oktyabrsky phonolites are intermediate members of the fluorophlogopite–phlogopite–hendricksite series. On the $KZn_3(AlSi_3O_{10})(OH)_2$–$KMn_3(AlSi_3O_{10})(OH)_2$ join there appears to be a limited solid solution extending from hendricksite to manganoan hendricksite and zincian shirozulite, with a miscibility gap close to the composition $KMn_3(AlSi_3O_{10})(OH)_2$. The Franklin Furnace hendricksite, showing the highest Mn content, is a member of this series.

Acknowledgements: The author thanks L.N. Pospelova, E.N. Nigmatulina, A.T. Titov, N.S. Karmanov, S.V. Kovyazin, S.Z. Smirnov (IGM, Novosibirsk), S.G. Simakin and Ye.V. Potapov (YBPTI, Yaroslavl) for their help with the EMPA, EDS and SIMS analyses of micas. The author is grateful to S.G. Kryvdik (IGMOF, Kiev) for his donation of the first phonolite samples used in the present work and guiding field trips to the Oktyabrsky massif. I.V. Pekov and A. Chakhmouradian are thanked for helpful comments on earlier versions of the manuscript. The last version of the manuscript was improved through comments and suggestions by editors R. Gieré and C. Ferraris and three anonymous reviewers. This work was partially supported by the project between Ukrainian National Academy of Sciences and Siberian Division of Russian Academy of Sciences ''Alkaline metasomatites of the Azov Sea and Baikal regions and their ore potential'' and the Russian Foundation for Basic Researches (grant 14-05-00391).

References

Abdalla, H., Matsueda, H., Ishihara, S., Miura, H. (1994): Mineral chemistry of albite-enriched granitoids at Um Ara, Southeastern Desert, Egypt. *Int. Geol. Rev.*, **36**, 1067–1077.

Armbruster, T., Richards, R., Gnos, E., Pettke, T., Herwegh, M. (2007): Unusual fibrous sodian tainiolite epitactic on phlogopite from marble xenoliths of Mont Saint-Hilaire, Quebec, Canada. *Can. Mineral.*, **45**, 541–549.

Brigatti, M.F. & Guggenheim, S. (2002): Mica crystal chemistry and the influence of pressure, temperature, and solid solution on atomistic models. *Rev. Mineral. Geochem.*, **46**, 1–97.

Brusnitsyn, A.I. & Nesterov, A.R. (2006): Shirozulite in manganese ore deposits of the South Urals, its chemical composition and the formulae of manganese micas. *Zapiski Vserossiyskogo Mineralogicheskogo Obshchestva*, **135**, 93–98. (in Russian with English abstract).

Chen, S. & Wu, G. (1987): Mineralogical study of Mn-biotite in miarolitic granite from Kuiqi, Fujian. *Dizhi Lun Ping (Geol. Rev.)*, **33**, 222–228. (in Chinese).

Choi, J., Komarneni, S., Grover, K., Katsuki, H., Park, M. (2009): Hydrothermal synthesis of Mn-mica. *Appl. Clay Sci.*, **46**, 69–72.

Chukhrov, F.B., ed. (1992): Minerals. Volume IV. Part 1. Phyllosilicates. Nauka Publishing, Moscow, 598 p. (in Russian).

Craig, J.R., Sandhaus, D.J., Guy, R.E. (1985): Pyrophanite, $MnTiO_3$, from Sterling Hill, New Jersey. *Can. Mineral.*, **23**, 491–494.

Dubina, A.V., Sharygin, V.V., Krivdik, S.G., Bondarenko, I.N. (2008): Mineralogical and geochemical features of agpaitic alkaline rocks of the Oktyabrsky massif, Ukraine. *in* Abstracts of 25th International conference ''Geochemistry of magmatic rocks'', School ''Alkaline magmatism of the Earth'', Saint-Petersburg-Moscow, ONTI GEOKHI, 47–48 (in Russian).

du Bray, E.A. (1994): Compositions of micas in peraluminous granitoids of the eastern Arabian Shield. Implications for petrogenesis and tectonic setting of highly evolved, rare-metal enriched granites. *Contrib. Mineral. Petrol.*, **116**, 381–397.

Dubyna, A.V., Kryvdik, S.G., Sharygin, V.V. (2014): Geochemistry of nepheline and alkaline syenites of the Ukrainian Shield (ICP-MS data). *Geochem. Int.*, **52**(10), 842–856.

Dumańska-Słowik, M., Sikorska, M., Heflik, W. (2011): Dissolved-recrystallized zircon from mariupolite in the Mariupol Massif, Priazovje (SE Ukraine). *Acta Geol. Pol.*, **61**(3), 277–288.

Dumańska-Słowik, M., Budzyń, B., Heflik, W., Sikorska, M. (2012): Stability relationships of REE-bearing phosphates in an alkali-rich system (nepheline syenite from the Mariupol Massif, SE Ukraine). *Acta Geol. Pol.*, **62**(2), 247–265.

Dumańska-Słowik, M., Wesełucha-Birczyńska, A., Pieczka, A. (2015): Micas from mariupolite of the Oktiabrski massif (SE Ukraine): An insight into the host rock evolution – Geochemical data supported by Raman microspectroscopy. *Spectrochim. Acta A: Mol. Biomol. Spectrosc.*, **137**, 817–826.

Evans, B.W. & Strens, R.G.J. (1966): Zinc mica from Franklin Furnace, New Jersey. *Nature*, **211**, 619–619.

Frondel, C. & Einaudi, M. (1968): Zinc-rich micas from Sterling Hill, New Jersey. *Am. Mineral.*, **53**, 1752–1754.

Frondel, C. & Ito, J. (1966): Hendricksite, a new species of mica. *Am. Mineral.*, **51**, 1107–1123.

Guggenheim, S., Schulze, W.A., Harris, G.A., Lin, J.-C. (1983): Noncentric layer silicates: An optical second harmonic generation, chemical and X-ray study. *Clays Clay Minerals*, **31**, 251–260.

Hazen, R.M. & Wones, D.R. (1972): The effect of cation substitutions on the physical properties of trioctahedral micas. *Am. Mineral.*, **57**, 103–129.

Ishida, K., Hawthorne, F.C., Hirowatari, F. (2004): Shirozulite, $KMn^{2+}{}_3(Si_3Al)O_{10}(OH)_2$, a new manganese-dominant trioctahedral mica: Description and crystal structure. *Am. Mineral.*, **89**, 232–238.

Jochum, K.P., Dingwell, D.B., Rocholl, A., Stoll, B., Hofmann, A.W., Becker, S., Besmehn, A., Bessette, D., Dietze, H.-J., Dulski, P., Erzinger, J., Hellebrand, E., Hoppe, P., Horn, I., Janssens, K., Jenner, G., Klein, M., McDonough, W.F., Maetz, M., Mezger, K., Münker, C., Nikogosian, I.K., Pickhart, C., Raczek, I., Rhede, D., Seufert, H.M., Simakin, S.G., Sobolev, A.V., Spettel, A.V., Straub, S., Vincze, L., Wallianos, A., Weckwerth, G., Weyer, S., Wolf, D., Zimmer, M. (2000): The preparation and preliminary characterisation of eight geological MPI-DING reference glasses for in-situ microanalysis. *Geostandard Newslett.*, **24**, 87–133.

Khomyakov, A.P., Cámara, F., Sokolova, E. (2010): Carbobystrite, $Na_8[Al_6Si_6O_{24}](CO_3)\cdot 4H_2O$, a new cancrinite-group mineral species from the Khibina alkaline massif, Kola Peninsula, Russia: description and crystal structure. *Can. Mineral.*, **48**, 291–300.

Komarneni, S. & Newalkar, B.L. (2003): Low-temperature synthesis of micas under conventional- and microwave-hydrothermal conditions. *Clays Clay Minerals*, **51**, 693–700.

Krivdik, S.G. & Tkachuk, V.I. (1988): Eudyalite-bearing agpaitic phonolites and dike nepheline syenites of the Oktyabrsky massif, Ukrainian Shield. *Geokhimiya*, **26**, 1133–1139. (in Russian).

—, — (1990): The petrology of alkaline rocks of the Ukrainian Shield. Naukova Dumka Publishing, Kiev, 408 p. (in Russian).

—, — (1998): Geochemical and petrological features of alkaline rocks of the Oktyabrsky massif, Ukraine. *Geokhimiya*, **36**, 362–371. (in Russian).

Kryvdik, S.G., Morgun, V.G., Sharygin, V.V. (2010): Micas of fenites and alkaline metasomatites from Eastern Azov Sea region. *Mineral. J. (Ukraine)*, **32**(4), 3–11. (in Ukrainian with English abstract).

Kryvdik, S.G., Sharygin, V.V., Morgun, V.G., Dubyna, O.V. (2013): Apoquartzite fenites of Eastern Azov Sea region (petrogoly, mineralogy, metallogeny). *Mineral. J. (Ukraine)*, **35**(4), 99–113. (in Ukrainian with English abstract).

Kryvdik, S.G., Sharygin, V.V., Amashukeli Yu, A., Dubyna, O.V. (2014): Chemical evolution of mafic minerals in alkaline rocks of Oktyabrsky massif (Azov area, Ukraine). *Mineral. J. (Ukraine)*, **36**(4), 5–19. (in Ukrainian with English abstract).

Lowell, R. & Ahl, M. (2000): Chemistry of dark zinnwaldite from Bom Futuro tin mine, Rondônia, Brazil. *Mineral. Mag.*, **64**, 699–709.

Melcher, F. (1995): Genesis of chemical sediments in Birimian greenstone belts: evidence from gondites and related manganese-bearing rocks from northern Ghana. *Mineral. Mag.*, **59**, 229–251.

Morozewicz, J. (1930): Der Mariupolit und seine Blutsverwandten. *Mineral. Petrogr. Mitt., Neue Folge*, **40**(5–6), 335–436.

Pekov, I.V. (2005): Genetic mineralogy and crystal chemistry of rare elements in high-alkaline postmagmatic systems. D.Sc. thesis, Moscow State University, Russia, 652 p. (in Russian).

Pekov, I.V., Chukanov, N.V., Ferraris, G., Ivaldi, G., Pushcharovsky, D.Yu., Zadov, A.E. (2003): Shirokshinite, $K(NaMg_2)Si_4O_{10}F_2$, a new mica with octahedral Na from Khibiny massif, Kola Peninsula: descriptive data and structural disorder. *Eur. J. Mineral.*, **15**, 447–454.

Pekov, I.V., Olysych, L.V., Chukanov, N.V., Zubkova, N.V., Pushcharovsky, D.Yu., Van, K.V., Giester, G., Tillmanns, E. (2011): Crystal chemistry of cancrinite group minerals with an *AB*-type framework: a review and new data. I. Chemical and structural variations. *Can. Mineral.*, **49**, 1129–1150.

Perrotta, A.J. & Garland, T.J. (1975): Low temperature synthesis of zinc-phlogopite. *Am. Mineral.*, **60**, 152–154.

Piilonen, P.C, Pekov, I.V., Back, M., Steede, T., Gault, R.A. (2006): Crystal-structure refinement of a Zn-rich kupletskite from Mont Saint-Hilaire, Québec, with contributions to the geochemistry of zinc in peralkaline environments. *Mineral. Mag.*, **70**, 565–578.

Pouchou, I. L. & Pichoir, F. (1985): ''PaP'' (phi-rho-z) procedure for improved quantitative microanalysis. *in* ''Microbeam Analysis'', I.T. Armstrong, ed. San Francisco Press, San Francisco, CA, 104–106.

Rieder, M., Cavazzini, G., D'yakonov, Yu.S., Frank-Kamenetskii, V.A., Gottardi, G., Guggenheim, S., Koval, P.V., Müller, G., Neiva, A.M.R., Radoslovich, E.W., Robert, J.-L., Sassi, F.P., Takeda, H., Weiss, Z., Wones, D.R. (1998): Nomenclature of the micas. *Can. Mineral.*, **36**, 905–912.

Robert, J.-L. & Gaspérin, M. (1985): Crystal structure refinement of hendricksite, a Zn- and Mn-rich trioctahedral potassium mica: a contribution to the crystal chemistry of zinc-bearing minerals. *Tscher. Miner.* Petrogr. *Mitt.,* **34**, 1–14.

Robert, J.-L. & Maury, R.C. (1979): Natural occurrence of a (Fe,Mg,Mn) tetrasilicic potassium mica. *Contrib. Mineral. Petrol.*, **68**, 117–123.

Shannon, R.D. (1976): Revised effective ionic radii and systematic studies of interatomic distances in halides and chalcogenides. *Acta Crystallogr.*, **A32**, 751–767.

Sharygin, V.V. (2009): New minerals and mineral species of the Azov region: Oktyabrsky massif. *Trans. UkrNDMI NAN Ukraine*, **5**(2), 132–139. (in Russian).

Sharygin, V.V. & Kryvdik, S.G. (2010): Behavior of Zn in late magmatic and metasomatic rocks of the Oktyabrsky alkaline massif, Azov region, Ukraine: mineralogical data. *in* Abstracts and excursion guide of conference dedicated to the memory of J.A. Morozewicz ''Alkaline rocks: petrology, mineralogy, geochemistry'', Kyiv, 58–59.

—, — (2014): New minerals in alkaline metasomatites at Dmitrovka, Azov Sea region, Ukraine. *in* Proceedings of 8th conference dedicated to the memory of academician E. Lazarenko ''Mineralogy: real and future'', Lviv-Carpathians, PH of Lviv National University, 167–170. (in Russian).

Sharygin, V.V., Krivdik, S.G., Pospelova, L.N., Dubina, A.V. (2009): Zn-kupletskite and hendricksite in the agpaitic phonolites of the Oktyabrskii massif, Azov region, Ukraine. *Dokl. Earth Sci.*, **425**, 499–504.

Sobachenko, V.N., Matveyeva, L.N., Khaltuyeva, V.K. (1989): The evolution of mica composition in granitization and near-fracture metasomatic processes in Precambrian trough structures. *Geol. Geofiz.*, **30**(12), 73–81. (in Russian).

Stone, M., Exley, C.S., George, M.C. (1988): Compositions of trioctahedral micas in the Cornubian batholith. *Mineral. Mag.*, **52**, 175–192.

Tischendorf, G., Förster, H.-J., Gottesmann, B. (2001): Minor- and trace-element composition of trioctahedral micas: a review. *Mineral. Mag.*, **65**, 249–276.

Tischendorf, G., Förster, H.-J., Gottesmann, B., Rieder, M. (2007): True and brittle micas: composition and solid-solution series. *Mineral. Mag.*, **71**, 285–320.

Tlili, A., Smith, D.C., Beny, J.-M., Boyer, H. (1989): A Raman microprobe study of natural micas. *Mineral. Mag.*, **53**, 165–179.

Tracy, R.J. (1991): Ba-rich micas from the Franklin Marble, Lime Crest and Sterling Hill, New Jersey. *Am. Mineral.*, **76**, 1683–1693.

Yoshii, M., Togashi, Y., Maeda, K. (1973): On the intensity changes of basal reflections with relation to barium content in manganoan phlogopites and kinoshitalite. *Bull. Geol. Surv. Japan*, **24**, 543–550.

Received 29 July 2014
Modified version received 21 February 2015
Accepted 3 April 2015